Dear Prof. Erwin Zehe:

Many thanks for your work. I have revised the manuscript again as you and the reviewer suggested. I accepted almost all of the reviewer's suggestions. Major revisions include: 1) I have removed almost all of the second part of the results sections as the reviewer suggested; 2) Table 4 was displaced into the supplement. I think the revisions can better streamline the paper. In addition, I added the *R* codes in the supplement.

Best regards

Mingguo Zheng

2020-3-29

Response to Reviewer

Many thanks for your comments. I accepted almost all of your suggestions this time. My responses are given as follows.

The new title "A mathematically precise method to partition climate and catchment effects on runoff" is less specific then the old one which I prefer.

I have revised the title as suggested.

The second part of the results sections is concerned with the sensitivities, which I think is not so strongly related to the main message of this paper. For the sake of brevity, I suggest to remove it. This would focus the paper, allow to reduce the number of figures and avoid possible distraction of the reader.

As suggested, I have removed all of the second part and only remained Fig. 8.

In my first review I suggested to remove or adapt the results of catchments 10,11 since these only have 3 years for their base period, while the evaluation period is > 10 yrs. This short period is probably insufficient to allow stationary conditions, which are essential for such a method. The argument of the author to keep these catchments only because they have been published by another paper does not help here.

As suggested, I have removed the catchments from the analyses and made revisions in all related tables, figures and texts.

Minor comments:

Figures 1-3 show different axes although I thought that they intend to show the same relationships. I suggest to make this more consistent.

I think the comments over, but I am sorry that the figures cannot have the same axes.

Figure 2: the annotation in the figure seems to be switched; also What represents the continuous lines?

Many thanks for your careful examination. The annotation was indeed switched. I have made revisions.

L653 “In this case, the integral path of the LI method can be considered as the broken line AB+BC in Fig. 3” There is no broken line in Fig.3

I have revised it as “path ABC”.

A line integral-based ~~mathematically precise~~ method to partition climate and catchment effects on runoff

Mingguo Zheng[1, 2*]

[1]National-Regional Joint Engineering Research Center for Soil Pollution Control and Remediation in South China, Guangdong Key Laboratory of Integrated Agro-environmental Pollution Control and Management, Guangdong Institute of Eco-environmental Science & Technology, Guangdong Academy of Sciences, Guangzhou 510650, China

[2]Guangdong Engineering Center of Non-point Source Pollution Prevention Technology, Guangzhou 510650, China

~~[1]Guangdong Key Laboratory of Integrated Agro-environmental Pollution Control and Management/ Guangdong Engineering Center of Non-point Source Pollution Prevention Technology, Guangdong Institute of Eco-environment Science & Technology, Guangzhou 510650, China~~

~~[2]National-Regional Joint Engineering Research Center for Soil Pollution Control and Remediation in South China, Guangzhou 510650, China;~~

Correspondence: Mingguo Zheng (mgzheng@soil.gd.cn)

Abstract

It is a common task to partition the synergistic impacts of drivers in the environmental sciences. However, there is no mathematically precise solution to this partition ~~process~~task. Here I presented a line integral-based method, which addresses the sensitivity to the drivers throughout the drivers' ~~ir~~ evolutionary paths so as to ensure a precise partition. The method reveals that the partition depends on both the change magnitude and pathway (timing of the change), but not on the magnitude alone unless used for a linear system. To illustrate this method, I ~~used~~ applied the Budyko framework to partition the effects of climatic and catchment conditions on the temporal change in the runoff for ~~21 catchments~~19 catchments from Australia and China. The proposed method reduces to the decomposition method when assuming a path in which climate change occurs first, followed by an abrupt change in catchment properties. The proposed method re-defines the widely-used sensitivity at a point as the path-averaged sensitivity. The total differential and the complementary methods simply concern the sensitivity at the initial or/and the terminal state, so they cannot give precise results. Although the path-averaged sensitivities varied greatly among the catchments, they can be readily predicted within the Budyko framework.~~The path-averaged sensitivity of water yield to climate conditions was found to be stable over time. Space-wise, moreover, the sensitivity can be readily predicted even in the absence of streamflow observations, which facilitates the evaluation of future climate effects on streamflow.~~ As a mathematically accurate solution, the proposed method provides a generic tool to conduct quantitative attribution analyses.

Keywords: Runoff; Climate change; Human activities; Attribution analysis; Budyko

带格式的: 缩进: 首行缩进: 0 字符

带格式的: 两端对齐

设置了格式: 字体: (中文) 宋体, 字体颜色: 黑色

设置了格式: 字体: (默认) Times New Roman, (中文) 宋体, 字体颜色: 黑色

设置了格式: 字体: (中文) 宋体, 字体颜色: 黑色

设置了格式: 字体: (默认) Times New Roman, (中文) Calibri, 字体颜色: 自动设置

设置了格式: 字体颜色: 自动设置

1 Introduction

The impacts of certain drivers on observed changes of interest often require quantification in environmental sciences. In the hydrology community, both climate and human activities have posed global-scale impact on hydrologic cycle and water resources (Barnett *et al.*, 2008; Xu *et al*., 2014; Wang and Hejazi, 2001). Diagnosing their relative contributions to runoff is of considerable relevance to the researchers and managers. Unfortunately, performing a quantitative attribution analysis of runoff changes remains a challenge (Wang and Hejazi, 2001; Berghuijs and Woods, 2016; Zhang *et al.*, 2016); this is to a considerable degree due to a lack of a mathematically precise method to decouple synergistic and often confounding impacts of climate change and human activities.

Numerous studies have detected the long-term variability in runoff and attempted to partition the effects of climate change and human activities through various methods (Dey and Mishra, 2017); these include the paired-catchments method and the hydrological modeling method. The paired-catchment method can filter the effect of climatic variability and thus isolate the runoff change induced by vegetation changes (Brown *et al.*, 2005). However, this method is capital intensive; moreover, it generally involves small catchments and experiences difficulties when extrapolating to large catchments (Zhang *et al.*, 2011). The physical-based hydrological models often have limitations such as a high data requirement, labor-intensive calibration and validation processes, and inherent uncertainty and interdependence in parameter estimations (Binley *et al.*, 1991; Wang *et al.*, 2013; Liang *et al.*, 2015). Conceptual models such as Budyko-type equations (see Section 2.1) have consequently gained interest in recent years ~~(see Section 2.1)~~.

Within the Budyko framework, studies (Roderick and Farquhar, 2011; Zhang *et al.*, 2016) have used the total differential of runoff as a proxy for the runoff change and the partial derivatives as the sensitivities (hereafter called the total differential method). The total differential, however, is simply a first-order approximation of the observed change (Fig. 1(a)). This approximation has caused an error in the calculation of climate impact on runoff, with the deviation ranging from 0 to 20 10^{-3}m (or -118 to 174%) in China (Yang *et al.*, 2014). The elasticity method proposed by Schaake (1990) is also based on the total differential expression (Sankarasubramanian *et al.*, 2001; Zheng *et al.*, 2009). The method uses the "elasticity" concept to assess the climate sensitivity of runoff. The elasticity coefficients, however, have been estimated in an empirical way and are not physically sound (Roderick and Farquhar, 2011; Liang *et al.*, 2015).

The so-called decomposition method developed by Wang and Hejazi (2011) has also been widely used. The method assumes that climate changes cause a shift along a Budyko curve and then human interferences cause a vertical shift from one Budyko curve to another (Fig. 2). Under this assumption, the method extrapolates the Budyko models that are calibrated using observations of the reference period, in which human impacts remain minimal, to determine the human-induced runoff changes that occur during the evaluation period.

Recently, Zhou *et al.* (2016) established a Budyko complementary relationship for runoff and further applied it to partitioning the climate and catchment effects. Superior to the total differential method, the complementary method culminates by yielding a no-residual partition. Nevertheless, this method depends on a given weighted factor that is determined in an empirical but not a precise way.

Furthermore, Zhou *et al.* (2016) argued that the partition is not unique in the Budyko framework because the path of the climate and catchment changes cannot be uniquely identified.

Obtaining a precise partition remains difficult, even when ~~using~~giving a precise mathematical model. This difficulty can be illustrated by using a precise hydrology model $R = f(x, y)$, where R represents runoff, and x and y represent the climate factors and catchment characteristics, respectively. We assumed that R changes by ΔR when x changed by Δx and y changes by Δy, *i.e.*, $\Delta R = f(x+\Delta x, y+\Delta y) - f(x, y)$. To determine the effect of x on ΔR, *i.e.* ΔR_x, a common practice is to assume that y remains constant when x changes by Δx. We thus obtain: $\Delta R_x = f(x+\Delta x, y) - f(x, y)$. Similarly, we can obtain: $\Delta R_y = f(x, y+\Delta y) - f(x, y)$. Although this derivation seems quite reasonable, it is problematic as $\Delta R_x + \Delta R_y \neq \Delta R$. A further examination shows that a variable's effect on R seems to differ depending on the changing path (timing of the change). For example, $\Delta R_x = f(x+\Delta x, y) - f(x, y)$ and $\Delta R_y = f(x+\Delta x, y+\Delta y) - f(x+\Delta x, y)$ if x changes first and y subsequently changes (Note that the partition is precise with $\Delta R_x + \Delta R_y = \Delta R$ at this moment). If y changes first and x subsequently changes, the partition then becomes: $\Delta R_x = f(x+\Delta x, y+\Delta y) - f(x, y+\Delta y)$ and $\Delta R_y = f(x, y+\Delta y) - f(x, y)$. In the case of x and y changing simultaneously, unfortunately, current literature seems not to provide a mathematically precise solution.

The aim of this study is to propose a mathematically precise method to conduct a quantitative attribution to drivers. The method is based on the line integer (called the LI method hereafter) and takes account of the sensitivity throughout the evolutionary path of the drivers rather than at a point as the total differential method does. ~~In this way, the proposed method revises the widely used concept of sensitivity at a point as the path-averaged sensitivity.~~ To present and evaluate the proposed method, I decomposed the relative influences of climate and catchment conditions on runoff within the Budyko framework using data from ~~21 catchments~~19 catchments from Australia and China. ~~I also examined the spatio-temporal variability of the path-averaged sensitivities and assessed their spatio-temporal predictability.~~

2 Methodology

2.1 Budyko Framework and the MCY equation

Budyko (1974) argued that the mean annual evapotranspiration (E) is largely determined by the water and energy balance of a catchment. Using precipitation (P) and potential evapotranspiration (E_0) as proxies for water and energy availabilities respectively, the Budyko framework relates evapotranspiration losses to the aridity index defined as the ratio of E_0 over P. The Budyko framework has gained wide acceptance in the hydrology community (Berghuijs and Woods, 2016; Sposito, 2017). In recent decades, several equations have been developed to describe the Budyko framework. Among them, the Mezentsev-Choudhury-Yang's equation (Mezentsev, 1955; Choudhury, 1999; Yang *et al.*, 2008) (Called the MCY equation hereafter) has been widely accepted and was used in this study:

$$\frac{E}{P}=\frac{E_0/P}{(1+(E_0/P)^n)^{1/n}} \qquad (1)$$

where $n\in(0,\infty)$ is an integration constant that is dimensionless, and represents catchment properties. Eq. (3) requires a relatively long time scale whereby the water storage of a catchment is negligible and the water balance equation reduces to be $R=P-E$. Here I adopted a "tuned" n value that can obtain an exact accordance between the calculated E by Eq. (1) and that actually encountered ($=P-R$).

The partial differentials of R with respect to P, E_0, and n are given as:

$$\frac{\partial R}{\partial P}=R_P(P,E_0,n)=1-\frac{E_0^{\,n+1}}{(P^n+E_0^{\,n})^{1/n}} \qquad (2a)$$

$$\frac{\partial R}{\partial E_0}=R_{E_0}(P,E_0,n)=-\frac{P^{n+1}}{(P^n+E_0^{\,n})^{1/n}} \qquad (2b)$$

$$\frac{\partial R}{\partial n}=R_n(P,E_0,n)=\frac{-E_0Pn^{-1}}{(P^n+E_0^{\,n})^{1/n}}\left[\frac{\ln(P^n+E_0^{\,n})}{n}-\frac{P^n\ln P+E_0^{\,n}\ln E_0}{P^n+E_0^{\,n}}\right] \qquad (2c)$$

2.2 Theory of the line integral-based method

We start by considering an example of a two-variable function $z=f(x, y)$ and assumed that x and y are independent. The function has continuous partial derivatives $\partial z/\partial x=f_x(x,y)$ and $\partial z/\partial y=f_y(x,y)$. Suppose that x and y vary along a smooth curve L (e.g. $\overset{\frown}{AC}$ in Fig. 3) from the initial state (x_0, y_0) to the terminal state (x_N, y_N), and z co-varies from z_0 to z_N. Let $\Delta z=z_N-z_0$, $\Delta x=x_N-x_0$, and $\Delta y=y_N-y_0$. Our goal is to determine a mathematical solution that quantifies the effects of Δx and Δy on Δz, *i.e.* Δz_x and Δz_y. Δz_x and Δz_y should be subject to the constraint $\Delta z_x+\Delta z_y=\Delta z$.

As shown in Fig. 3, points $M_1(x_1, y_1),\ldots, M_{N-1}(x_{N-1}, y_{N-1})$ partition L into N distinct segments. Let $\Delta x_i=x_{i+1}-x_i$, $\Delta y_i=y_{i+1}-y_i$, and $\Delta z_i=z_{i+1}-z_i$. For each segment, Δz_i can be approximated as dz_i: $\Delta z_i\approx \mathrm{d}z_i=f_x(x_i,y_i)\Delta x_i+f_y(x_i,y_i)\Delta y_i$. We then have: $\Delta z=\sum_{i=1}^{N}\Delta z_i\approx\sum_{i=1}^{N}f_x(x_i,y_i)\Delta x_i+\sum_{i=1}^{N}f_y(x_i,y_i)\Delta y_i$. We thus obtain the following respective approximation of Δz_x and Δz_y: $\Delta z_x\approx\sum_{i=1}^{N}f_x(x_i,y_i)\Delta x_i$ and $\Delta z_y\approx\sum_{i=1}^{N}f_y(x_i,y_i)\Delta y_i$. Next, define τ as the maximum length ~~among~~ of the N segments. The smaller the value of τ, the closer to Δz_i the value of dz_i, and then the more accurate the approximations are. The approximations become exact in the limit $\tau\to 0$. Taking the limit $\tau\to 0$ then converts the sum into integrals and gives a precise expression (this is an informal derivation and please see Appendix A for a formal one): $\Delta z=\lim_{\tau\to 0}\sum_{i=1}^{N}f_x(x_i,y_i)\Delta x_i+\lim_{\tau\to 0}\sum_{i=1}^{N}f_y(x_i,y_i)\Delta y_i=\int_L f_x(x,y)dx+\int_L f_y(x,y)dy$, where $\int_L f_x(x,y)dx=\lim_{\tau\to 0}\sum_{i=1}^{N}f_x(x_i,y_i)\Delta x_i$ and $\int_L f_y(x,y)dy=\lim_{\tau\to 0}\sum_{i=1}^{N}f_y(x_i,y_i)\Delta y_i$ denote the line integral of f_x and f_y

along L (termed integral path) with respect to x and y, respectively. $\int_L f_x(x,y)dx$ and $\int_L f_y(x,y)dy$ exist provided that f_x and f_y are continuous along L. We thus obtain a precise evaluation of Δz_x and Δz_y:

$$\Delta z_x = \int_L f_x(x,y)\mathrm{d}x \qquad (3a)$$

$$\Delta z_y = \int_L f_y(x,y)\mathrm{d}y\,. \qquad (3b)$$

Unlike the total differential method, the sum of Δz_x and Δz_y persistently equals Δz (Appendix B). If $f(x, y)$ is linear, then f_x and f_y are constant. Defining $f_x(x, y)$ and $f_y(x, y)$ remain constant at C_x and C_y respectively, then $\Delta z_x = C_x\Delta x$ and $\Delta z_y = C_y\Delta y$. Δz_x and Δz_y are thus independent of L. If $f(x, y)$ is non-linear, however, both Δz_x and Δz_y vary with L, as is exemplified in Appendix C. Hence, the initial and the terminal states, together with the path connecting them, determine the resultant partition unless $f(x, y)$ is linear.

The mathematical derivation above applies to a three-variable function as well. By doing the line integrals for the MCY equation, we obtain the desired results:

$$\Delta R_P = \int_L \frac{\partial R}{\partial P}\mathrm{d}P \qquad (4a)$$

$$\Delta R_{E_0} = \int_L \frac{\partial R}{\partial E_0}\mathrm{d}E_0 \qquad (4b)$$

$$\Delta R_n = \int_L \frac{\partial R}{\partial n}\mathrm{d}n \qquad (4c)$$

where ΔR_p, ΔR_{E_0}, and ΔR_n denote the effects on runoff change of P, E_0, and n, respectively. The sum of ΔR_p and ΔR_{E_0} represents the effect of climate change, and ΔR_n is often related to human activities although it probably includes the effects of other factors, such as climate seasonality (Roderick and Farquhar, 2011; Berghuijs and Woods, 2016). L denotes a three-dimensional curve along which climate and catchment changes have occurred. I approximated L by a series of line segments. ΔR_p, ΔR_{E_0}, and ΔR_n were finally determined by summing up the integrals along each of the line segments (see Section 2.3).

2.3 Using the LI method to determine ΔR_p, ΔR_{E_0}, and ΔR_n within the Budyko Framework

1) Determining ΔR_p, ΔR_{E_0}, and ΔR_n assuming a linear integral path

~~A curve can be approximated as a series of line segments.~~A curve can always be approximated as a series of line segments. Hence, we can first handle the case of a linear integral path. Given two consecutive periods and assuming that the catchment state has evolved from (P_1, E_{01}, n_1) to (P_2, E_{02}, n_2) along a straight line L, let $\Delta P = P_2 - P_1$, $\Delta E_0 = E_{02} - E_{01}$, and $\Delta n = n_2 - n_1$; then the line L is given by parametric equations: $P = \Delta Pt + P_1$, $E_0 = \Delta E_0 t + E_{01}$, $n = \Delta nt + n_1$, $t \in [0,1]$. Given these equations, Eq. (2) becomes a univariate function of t, *i.e.*, $\partial R/\partial P = R_P(t)$, $\partial R/\partial E_0 = R_{E_0}(t)$, and $\partial R/\partial n = R_n(t)$. Then, ΔR_P, ΔR_{E_0}, and ΔR_n can be evaluated as:

$$\Delta R_P = \int_L \frac{\partial R}{\partial P}\mathrm{d}P = \int_0^1 R_P(t)\mathrm{d}(\Delta Pt + P_1) = \Delta P\int_0^1 R_P(t)\mathrm{d}t \qquad (5a)$$

设置了格式: 字体: 小四

带格式的: 缩进: 首行缩进: 3.5 字符

设置了格式: 字体: (默认) Times New Roman, (中文)

$$\Delta R_{E_0} = \int_L \frac{\partial R}{\partial E_0} \mathrm{d}E_0 = \int_0^1 R_{E_0}(t)\mathrm{d}(\Delta E_0 t + E_{01}) = \Delta E_0 \int_0^1 R_{E_0}(t)\mathrm{d}t \qquad (5b)$$

$$\Delta R_n = \int_L \frac{\partial R}{\partial n} \mathrm{d}n = \int_0^1 R_n(t)\mathrm{d}(\Delta n t + n_1) = \Delta n \int_0^1 R_n(t)\mathrm{d}t \qquad (5c)$$

Unfortunately, I could not determine the antiderivatives of $R_P(t)\mathrm{d}t$, $R_{E_0}(t)\mathrm{d}t$ and $R_n(t)\mathrm{d}t$ and had to make approximate calculations. As the discrete equivalent of integration is a summation, we can approximate the integration as a summation. I divided the $t \in [0,1]$ interval into 1000 subintervals of the same width, *i.e.*, setting d*t* identically equal to 0.001, and then calculated $R_P(t)\mathrm{d}t$, $R_{E_0}(t)\mathrm{d}t$ and $R_n(t)\mathrm{d}t$ for each subinterval. Let $t_i = 0.001i$ ~~-~~, $i \in [0,999]$ and is integer-valued~~.~~; ΔR_P, ΔR_{E_0}, and ΔR_n are approximated as:

域代码已更改

$$\Delta R_P \approx 0.001 \Delta P \sum_{i=0}^{999} R_P(t_i) \qquad (6a)$$

$$\Delta R_{E_0} \approx 0.001 \Delta E_0 \sum_{i=0}^{999} R_{E_0}(t_i) \qquad (6b)$$

$$\Delta R_n \approx 0.001 \Delta n \sum_{i=0}^{999} R_n(t_i) \qquad (6c)$$

2) Dividing the evaluation period into a number of subperiods

I first determined a change point and divided the whole observation period into the reference and evaluation periods. To determine the integral path, the evaluation period was further divided into a number of subperiods. The Budyko framework assumes a steady state condition of a catchment and therefore requires no change in soil water storage. Over a time period of 5-10 years, it is reasonable to assume that changes in soil water storage will be sufficiently small (Zhang *et al.*, 2001). Here, I divided the evaluation period into a number of 7-year subperiods with the exception for the final subperiod, which varied from 7 to 13 years in length depending on the length of the evaluation period.

~~3)~~ 3) Determining ΔR_P, ΔR_{E_0}, and ΔR_n by approximating the integral path as a series of line segments

带格式的：无项目符号或编号

~~A curve can be approximated as a series of line segments.~~ For a short period, the integral path *L* can be considered as linear, which implies a temporally invariant change rate. For a long period in which the change rate ~~may~~ var~~y~~ies over time, *L* can be fitted using a number of line segments. Given a reference period and an evaluation period comprising *N* subperiods, ~~I assumed that~~ the catchment state was assumed to evolve~~d~~ from (P_0, E_{00}, n_0), …, (P_i, E_{0i}, n_i), …, to (P_N, E_{0N}, n_N), where the subscript "0" denotes the reference period, and "*i*" and "*N*" denote the *i*th and the final subperiods of the evaluation period, respectively. I used a series of line segments L_1, L_2, …, L_N to approximate the integral path *L*, where L_i connects points (P_{i-1}, $E_{0,i-1}$, n_{i-1}) with (P_i, E_{0i}, n_i). Then ΔR_P, ΔR_{E_0}, and ΔR_n were evaluated as the sum of the integrals along each of the line segments, which were calculated using Eq. (6).

2.4 Total-differential, decomposition and complementary methods

To evaluate the LI method, I compared it with the existing methods, including the decomposition method, the total differential method, and the complementary method. The total differential method approximated ΔR as d*R*:

$$\Delta R \approx \mathrm{d}R = \frac{\partial R}{\partial P}\Delta P + \frac{\partial R}{\partial E_0}\Delta E_0 + \frac{\partial R}{\partial n}\Delta n = \lambda_P \Delta P + \lambda_{E_0}\Delta E_0 + \lambda_n \Delta n \qquad (7)$$

where $\lambda_P = \partial R/\partial P$, $\lambda_{E_0} = \partial R/\partial E_0$, and $\lambda_n = \partial R/\partial n$, representing the sensitivity coefficient of R with respect to P, E_0, and n, respectively. Within the total differential method, $\Delta R_P = \lambda_P \Delta P$, $\Delta R_{E_0} = \lambda_{E_0}\Delta E_0$, and $\Delta R_n = \lambda_n \Delta n$. I used the forward approximation, *i.e.*, substituting the observed mean annual values of the reference period into Eq. (2), to estimate λ_P, λ_{E_0}, and λ_n, as is standard in most studies (Roderick and Farquhar, 2011; Yang and Yang, 2011; Sun *et al.*, 2014).

The decomposition method (Wang and Hejazi, 2011) calculated ΔR_n as follows:

$$\Delta R_n = R_2 - R_2^{'} = (P_2 - E_2) - (P_2 - E_2^{'}) = E_2^{'} - E_2 \qquad (8)$$

where R_2, P_2, and E_2 represents the mean annual runoff, precipitation and evapotranspiration of the evaluation period, respectively; $R_2^{'}$ and $E_2^{'}$ represent the mean annual runoff and evapotranspiration, respectively, given the climate conditions of the evaluation period and the catchment conditions of the reference period (Fig. 2). Both E_2 and $E_2^{'}$ were calculated by Eq. (1), but using n values of the evaluation period and the reference period respectively.

The complementary method (Zhou *et al.*, 2016) uses a linear combination of the complementary relationship for runoff to determine ΔR_P, ΔR_{E_0}, and ΔR_n:

$$\begin{aligned}\Delta R = {} & a\left[\left(\frac{\partial R}{\partial P}\right)_1 \Delta P + \left(\frac{\partial R}{\partial E_0}\right)_1 \Delta E_0 + P_2 \Delta\left(\frac{\partial R}{\partial P}\right) + E_{0,2}\Delta\left(\frac{\partial R}{\partial E_0}\right)\right] \\ & +(1-a)\left[\left(\frac{\partial R}{\partial P}\right)_2 \Delta P + \left(\frac{\partial R}{\partial E_0}\right)_2 \Delta E_0 + P_1 \Delta\left(\frac{\partial R}{\partial P}\right) + E_{0,1}\Delta\left(\frac{\partial R}{\partial E_0}\right)\right]\end{aligned} \qquad (9)$$

where the subscript 1 and 2 denotes the reference and the evaluation periods, respectively. a is a weighting factor and varies from 0 to 1. As suggested by Zhou *et al.* (2016), I set a = 0.5. Equation (9) thus gave an estimation of ΔR_P, ΔR_{E_0}, and ΔR_n as follows:

$$\Delta R_P = 0.5\Delta P\left[\left(\frac{\partial R}{\partial P}\right)_1 + \left(\frac{\partial R}{\partial P}\right)_2\right] \qquad (10a)$$

$$\Delta R_{E_0} = 0.5\Delta E_0\left[\left(\frac{\partial R}{\partial E_0}\right)_1 + \left(\frac{\partial R}{\partial E_0}\right)_2\right] \qquad (10b)$$

$$\Delta R_n = 0.5\Delta\left(\frac{\partial R}{\partial P}\right)(P_1 + P_2) + 0.5\Delta\left(\frac{\partial R}{\partial E_0}\right)(E_{0,1} + E_{0,2}) \qquad (10c)$$

2.5 Data

I collected runoff and climate data from ~~21~~ 19 selected catchments evaluated in previous studies (Table 1). The change-point years given in these studies were directly used to determine the reference and evaluation periods for the LI method. As mentioned above, the LI method further divides the evaluation period into a number of subperiods. For the sake of comparison, the final subperiod of the evaluation period was used as the evaluation period for the decomposition, the total differential and the complementary methods (It can be equally considered that all of the four methods used the final subperiod as the evaluation period, but the LI method cares about the intermediate period between the reference and the evaluation periods and the other methods do not). ~~Nine~~Eight of the ~~21 catchments~~19

设置了格式: 字体: (默认) Times New Roman, (中文)

catchments had a reference period comprising only one subperiod (Table 1), and the others had two to seven subperiods.

The ~~21~~ 19 selected catchments have diverse climates and landscapes with ~~14~~ 12 from Australia and seven from China (Table 1). The catchments span from tropical to subtropical and temperate areas and from humid to semi-humid and semiarid regions, with the mean annual rainfall varying from 506 to 1014 10^{-3}m and potential evaporation from 768 to 1169 10^{-3}m. The dryness index ranges between 0.86 and 1.91. The catchment areas vary by five orders of magnitude from 1.95 to 121,972 with a median 606 10^{6}m^{2}. The key data includes annual runoff, precipitation, and potential evaporation. The record length varied between ~~15~~ 19 and ~~75~~ 76 with a median of ~~35~~ 39 years. All the catchments experienced changes in climate and catchment properties over the observation periods. ~~Among the 21 catchments, t~~The precipitation changes from the reference to the evaluation period ranged between -153~~271~~ and 79 10^{-3}m yr^{-1} ~~for precipitation~~, and between -35 and 41 10^{-3}m yr^{-1} for potential evaporation (Table 2). The coeval change in the parameter n of the MCY equation ranged between -0.2 to ~~2.53~~1.4. ~~All the catchments experienced changes in climate and catchment properties over the observation periods.~~ The mean annual streamflow reduced for all catchments, ranging from 0.4~~3~~ to ~~229~~ 169 with a median 38 10^{-3}m yr^{-1}. ~~For all catchments, t~~The change in catchment properties mainly refer to the vegetation cover or land use change. More details of data and the catchments can be found in Zhang *et al.* (2011), Sun *et al.* (2014), Zhang *et al.* (2010), Zheng *et al.* (2009), Jiang *et al.* (2015), and Gao *et al.* (2016).

3 Results

~~3.1 Comparisons with existing methods~~

Table 3 lists the resultant values of ΔR_P, ΔR_{E_0}, and ΔR_n from the LI method and the three other methods. Please see the supplemental information section for detailed calculation steps.

Fig. 4(a) compares the resultant ΔR_n of the LI method and the decomposition method. Although they are quite similar, the discrepancies ~~between these values~~ can be up to >20 10^{-3}m yr^{-1}. The decomposition method assumes that climate change occurs first and then human interferences cause a sudden change in catchment properties (Fig. 2). Such a fictitious path is identical to the path ~~broken line of~~ AB~~+B~~C in Fig. 3, provided that x represents climate factors and y catchment properties. When adopting ABC as the integral path, the LI method yielded the same results as the decomposition method did (Fig. 4(b)). Hence~~As a result~~, the decomposition method can be considered as a ~~special~~ case of the LI method that uses a special integral path.

~~when adopting the AB+BC broken line in Fig. 3 as the integral path, as was demonstrated clearly in Fig. 4(b).~~

The total differentiae method is predicated on an approximate equation, *i.e.* Eq. (7). The LI method reveals that the precise form of the equation is $\Delta R = \overline{\lambda_P}\Delta P + \overline{\lambda_{E_0}}\Delta E_0 + \overline{\lambda_n}\Delta n$ (Appendix D), where $\overline{\lambda_P}$, $\overline{\lambda_{E_0}}$ and $\overline{\lambda_n}$ ~~(Table 4)~~ denote the path-averaged sensitivity of R to P, E_0, and n, respectively. All points along the path have the same weight in determining $\overline{\lambda_P}$, $\overline{\lambda_{E_0}}$ and $\overline{\lambda_n}$. To determine them, the total differential and the complementary methods utilize only the initial or/and the terminal states. Neglecting

设置了格式: 字体: (默认) Times New Roman, (中文)

设置了格式: 字体: (默认) Times New Roman, (中文)

设置了格式: 字体: (默认) Times New Roman, (中文) 宋体, 字体颜色: 黑色

设置了格式: 字体: (中文) 宋体, 字体颜色: 黑色

the intermediate states ~~would~~ results in an imprecise partition, as was illustrated in Fig. 1 using a univariate function, and even a reverse trend estimation (see ΔR_{E_0} for Catchment NO. 1 in Table 3).

~~Superior to the total differential method, the sum of ΔR_P, ΔR_{E_0}, and ΔR_n always equaled to ΔR for the LI method. Examination of the subperiods revealed that $\partial R/\partial n$ was more temporally variable than $\partial R/\partial P$ and $\partial R/\partial E_0$ (discussed below). For this reason, ΔR_n showed considerable discrepancies between the two methods, but ΔR_P as well as ΔR_{E_0} matched closely between the two methods (Fig. 5).~~

As with the LI method, the complementary method produced ΔR_P, ΔR_{E_0}, and ΔR_n that exactly summed up to ΔR. Although its resultant ΔR_P, ΔR_{E_0}, and ΔR_n values were all in accordance with the LI method (Fig. 6), the LI method often yielded values beyond the bounds given by the complementary method (Fig. 7); this is because the maximum or minimum sensitivities do not necessarily occur at the initial or terminal states.

带格式的: 段落间距段前: 0 磅

~~3.2 Spatio-temporal variability of the path-averaged sensitivities~~

$\overline{\lambda_P}$, $\overline{\lambda_{E_0}}$ and $\overline{\lambda_n}$ imply the average runoff change induced by a unit change in P, E_0 and n, respectively (Appendix D). ~~Their spatio-temporal variability is relevant to the prediction of the runoff change. To evaluate their temporal variabilities, I calculated $\overline{\lambda_P}$, $\overline{\lambda_{E_0}}$ and $\overline{\lambda_n}$ for each subperiod of the evaluation period and assessed their deviation from those for the whole evaluation period. As shown in Fig. 8, the deviation was rather limited for $\overline{\lambda_P}$ (averaged 8.6%) and $\overline{\lambda_{E_0}}$ (averaged 13%), but was considerable for $\overline{\lambda_n}$ (averaged 41%). Hence, it seems quite safe to predict the future climate effects on runoff using the earlier $\overline{\lambda_P}$ and $\overline{\lambda_{E_0}}$ values, but care must be taken when using earlier $\overline{\lambda_n}$ to predict future catchment effect.~~

~~Different from the temporal variability,~~ $\overline{\lambda_P}$, $\overline{\lambda_{E_0}}$ and $\overline{\lambda_n}$ all varied by up to several times or even ten folds between the studied catchments (~~Table~~ Table S4~~4~~). ~~Strong correlations were observed between $\overline{\lambda_P}$ and P, between $\overline{\lambda_{E_0}}$ and P, and between $\overline{\lambda_n}$ and n (Fig. 9).~~ Fig. ~~10~~ 8 shows that Eq. (2) reproduced $\overline{\lambda_P}$, $\overline{\lambda_{E_0}}$ and $\overline{\lambda_n}$ very well taking the long-term means of P, E_0, and n as inputs, a fact that the dependent variable approached its average if the independent variables were set to be their averages. This finding is of relevance to the spatial prediction of $\overline{\lambda_P}$, $\overline{\lambda_{E_0}}$ and $\overline{\lambda_n}$.

~~Runoff data and, in turn, the parameter n in the MCY equation are often unavailable. It is thus desirable to make predictions of $\overline{\lambda_P}$, $\overline{\lambda_{E_0}}$ and $\overline{\lambda_n}$ in the absence of the parameter n. I developed three strategies as follows: 1) using Eq. (2) and assuming $n = 2$ as n is typically in a small range from 1.5 to 2.6 (Roderick and Farquhar, 2011); 2) using P and E_0 to establish regression models; 3) using the aridity index to establish regressions as the index appeared to be more strongly correlated with both $\overline{\lambda_P}$ and $\overline{\lambda_{E_0}}$ than P and E_0 (Fig. 9). As shown in Fig. 11, the three strategies show similar performance although the second one seems to perform better. All the strategies gave acceptable predictions of $\overline{\lambda_P}$ and $\overline{\lambda_{E_0}}$ but poor results for $\overline{\lambda_n}$, as it was primarily controlled by n (Fig. 9). Thus, more sophisticated approaches are needed to predict the future catchment effect on runoff in the absence of runoff observations.~~

4 Discussion

The LI method highlights the role of the evolutionary path in determining the resultant partition. Yet, it seems that no studies have accounted for the path issue while evaluating the relative influences of drivers. The limit of the LI method is high data requirement for obtaining the evolutionary path. When the path data are unavailable, the complementary method can be considered as an alternative. The complementary method is free of residuals; moreover, it employs both data of the reference and the evaluation periods, thereby generally yielding sensitivities closer to the path-averaged results than the total differentiae method.

While using the Budyko models, a reasonable time scale is relevant to meet the assumption that changes in catchment water storage are small relative to the magnitude of fluxes of P, R and E (Donohue *et al*., 2007; Roderick and Farquhar, 2011). A seven-year time scale was used in the present study, as most studies have suggested that a time period of 5-10 years (Zhang *et al*., 2001; Zhang *et al*., 2016; Wu *et al*., 2017a; Wu *et al*., 2017b; Li *et al*., 2017) or even one year (Roderick and Farquhar, 2011; Sivapalan *et al*., 2011; Carmona *et al*., 2014; Ning *et al*., 2017) is reasonable. Nevertheless, some studies argued that the time period should be longer than ten years (Li *et al*., 2016; Dey and Mishra, 2017). ~~If this is the case, the high temporal variation of~~ $\cancel{\overline{\lambda_n}}$ ~~shown in Fig. 8 might be caused by water storage changes, rather than actual changes in the catchment properties. This uncertainty should be addressed.~~ Using the Gravity Recovery and Climate Experiment (GRACE) satellite gravimetry, Zhao *et al*. (2011) detected the water storage variations for three largest river basins of China, namely, the Yellow, Yangtze, and Zhujiang. The Yellow River mostly drains an arid and semiarid region (P, 450 10^{-3}m; R, 70 10^{-3}m; E, 380 10^{-3}m), and the Yangtze (P, 110 10^{-3} m; R, 550 10^{-3}m; E, 550 10^{-3}m) and the Zhujiang river basins (P, 1400 10^{-3}m; R, 780 10^{-3}m ; E, 620 10^{-3}m) are humid. The amplitude of the water storage variations between years were 7, 37.2, and 65 10^{-3}m for the three rivers respectively, at one magnitude order smaller than the fluxes of P, R and E. Although the observations cannot be directly extrapolated to other regions, the possibility seems remote that the use of a 7-year aggregated time strongly violates the assumption of the steady state condition.

The mutual independence between the drivers is crucial for a valid partition. In the present study, although annual P and E_0 exhibited significant correlation for most catchments (p<0.05), the aggregated P, E_0 and n over a 7-year period showed minimal correlation (mostly p>0.1). The interdependence between the drivers can considerably confound the resultant partitions of the LI method and other existing methods.

The LI method re~~define~~vises the ~~widely used~~ concept of sensitivity at a point as the path-averaged sensitivity. Mathematically, the LI method is unrelated to a functional form and hence applies to communities other than just hydrology. For example, identifying the carbon emission budgets (an allowable amount of anthropogenic CO_2 emission consistent with a limiting warming target), is crucial for global efforts to mitigate climate change. The LI method suggested that the emission budgets depends on both the emission magnitude and pathway (timing of emissions), which is in line with a recent study by Gasser *et al.* (2018). ~~Hence, a~~An optimal pathway would facilitate an elevated carbon budget unless the carbon-climate system behaves in a linear fashion.

This study presented the LI method using time-series data, but it applies equally to the case of spatial series of data. Given a model that relates fluvial or aeolian sediment load to the influencing

带格式的: 段落间距段前: 0 磅

factors (e.g. rainfall and topography), for example, the LI method can be used to separate their contributions to the sediment-load change along a river or in the along-wind direction.

5 Conclusions

Based on the line integral, I created a mathematically precise method to partition the synergistic effects of several factors that cumulatively drive a system to change from a state to the other. The method is relevant for quantitative assessments of the relative roles of the factors on the change in the system state. I applied the LI method to partition the effects of climatic and catchment conditions on runoff within the Budyko framework. The method reveals that in addition to the change magnitude, the change pathways of climatic and catchment conditions also play a role~~control their impacts on runoff~~. Instead of using the runoff sensitivity at a point, the LI method uses the path-averaged sensitivity, thereby ensuring a mathematically precise partition. ~~I further examined the spatio-temporal variability of the path-averaged sensitivity. Time-wise, the runoff sensitivity to climate is stable but that to catchment properties is highly variable, suggesting that predicting future climate effects using earlier observations is reliable but care must be taken when predicting future catchment effects. Space-wise (between catchments) the runoff sensitivity both to climatic and catchment conditions was highly variable, but it can be accurately depicted by long-term means of the climatic and catchment conditions.~~ As a mathematically accurate scheme, the LI method has the potential to be a generic attribution approach in the environmental sciences.

Data availability

The data used in this study are freely available by contacting the authors.

Author contribution

MZ designed the study, analyzed the data and wrote the manuscript.

Competing interests

The authors declare that they have no conflict of interest.

Appendix A: Mathematical proof of $\Delta z = \int_L f_x(x,y)dx + \int_L f_y(x,y)dy$

We define that the curve L in Fig. 3 is given by a parametric equation: $x = x(t)$, $y = y(t)$, $t \in [t_0, t_N]$, then $\Delta z = z_N - z_0 = f[x(t_N), y(t_N)] - f[x(t_0), y(t_0)]$. Substituting the parametric equations, we obtain:

The right-hand side of the equation$= \int_L f_x(x,y)dx + \int_L f_y(x,y)dy$

$$= \int_{t_0}^{t_N} f_x[x(t), y(t)]\mathrm{d}x(t) + \int_{t_0}^{t_N} f_y[x(t), y(t)]\mathrm{d}y(t)$$

$$= \int_{t_0}^{t_N} \left\{ f_x[x(t), y(t)]x'(t) + f_y[x(t), y(t)]y'(t) \right\} \mathrm{d}t \qquad \text{(A1)}$$

Let $g(t) = f[x(t), y(t)]$, and after using the chain rule to differentiate g with respect to t, we obtain:

$$g'(t) = \frac{\partial g}{\partial x}\frac{\mathrm{d}x}{\mathrm{d}t} + \frac{\partial g}{\partial y}\frac{\mathrm{d}y}{\mathrm{d}t} = f_x[x(t), y(t)]x'(t) + f_y[x(t), y(t)]y'(t) \qquad \text{(A2)}$$

Thus, $g'(t)$ is just the integrand in Eq. (A1), and Eq. (A1) can then be rewritten as:

The right-hand side of the equation $= \int_{t_0}^{t_N} g'(t)\,\mathrm{d}t = \left[g(t)\right]_{t_0}^{t_N} = g(t_N) - g(t_0)$ $= f[x(t_N), y(t_N)] - f[x(t_0), y(t_0)] =$ The left-hand side of the equation

Appendix B: The sum of $\int_L f_x(x, y)\mathrm{d}x$ and $\int_L f_y(x, y)\mathrm{d}y$ is path-independent

Theorem: Given an open simply-connected region G (*i.e.*, no holes in G) and two functions $P(x, y)$ and $Q(x, y)$ that have continuous first-order derivatives, if and only if $\partial P / \partial y = \partial Q / \partial x$ throughout G, then $\int_L P(x, y)\mathrm{d}x + \int_L Q(x, y)\mathrm{d}y$ is path independent, *i.e.*, it depends solely on the starting and ending point of L.

We have $\partial f_x / \partial y = \partial^2 z / \partial x \partial y$ and $\partial f_y / \partial x = \partial^2 z / \partial y \partial x$. As $\partial^2 z / \partial x \partial y = \partial^2 z / \partial y \partial x$, we can state that $\partial f_x / \partial y = \partial f_y / \partial x$, meeting the above condition and proving that $\int_L f_x(x, y)\mathrm{d}x + \int_L f_y(x, y)\mathrm{d}y$ is path independent. The statement was further exemplified using a fictitious example in Appendix C.

Appendix C: A fictitious example to show how the LI method works

Runoff (R, 10^{-3}m yr^{-1}) at a site is assumed to increase from 120 to 195 10^{-3}m yr^{-1} with ΔR = 75 10^{-3}m yr^{-1}; meanwhile, precipitation (P, 10^{-3} m yr^{-1}) varies from 600 to 650 10^{-3}m yr^{-1} (ΔP = 75 10^{-3}m yr^{-1}) and the runoff coefficient (C_R, dimensionless) varies from 0.2 to 0.3 (ΔC_R = 0.1). The goal is to partition ΔR into the effects of the precipitation (ΔR_P) and runoff coefficient (ΔR_{C_R}), provided that P and C_R are independent. We have a function $R = PC_R$ and its partial derivatives $\partial R / \partial P = C_R$ and $\partial R / \partial C_R = P$. Given a path L along which P and C_R change and using Eq. (3), the LI method evaluates ΔR_P and ΔR_{C_R} as:

$$\Delta R_{C_R} = \int_L \partial R / \partial C_R \mathrm{d}C_R = \int_L P\mathrm{d}C_R \text{ and } \Delta R_P = \int_L \partial R / \partial P \mathrm{d}P = \int_L C_R \mathrm{d}P \qquad \text{(C1)}$$

带格式的: 缩进: 左侧: 0.63 厘米, 段落间距段后: 0 磅

The result differs depending on L but the sum of ΔR_P and ΔR_{C_R} uniformly equals ΔR. This dynamic is demonstrated using Fig. 3, in which we considered that the x-axis represents C_R and the y-axis P. Point A denotes the initial state (C_R = 0.2, P = 600) and point C the terminal state (C_R = 0.3, P = 650). I calculated ΔR_P and ΔR_{C_R} along three fictitious paths as follows:

1) L=AC. Line segment AC has equation $P = 500C_R + 500$, $0.2 \le C_R \le 0.3$. Let's take C_R as the parameter and write the equation in the parametric form as $P = 500C_R + 500$, $C_R = C_R$, $0.2 \le C_R \le 0.3$. By substituting the equation into Eq. (C1), we have:

$$\Delta R_{C_R} = \int_{AC} P\mathrm{d}C_R = \int_{0.2}^{0.3} (500C_R + 500)\mathrm{d}C_R = 62.5$$

$$\Delta R_P = \int_{AC} C_R \mathrm{d}P = \int_{AC} C_R \mathrm{d}(500C_R + 500) = 500\int_{0.2}^{0.3} C_R \mathrm{d}C_R = 12.5$$

2) L=AB+BC. To evaluate on the broken line, we can evaluate separately on AB and BC and then sum them up. The equation for AB is P = 600, $0.2 \le C_R \le 0.3$, while for BC is C_R = 0.3, $600 \le P \le 650$. Notes that a constant C_R or P implies that dC_R = 0 or dP = 0. Eq. (C1) then becomes:

$$\Delta R_{C_R} = \int_{AB+BC} P \mathrm{d}C_R = \int_{AB} P \mathrm{d}C_R + \int_{BC} P \mathrm{d}C_R = \int_{0.2}^{0.3} 600 \mathrm{d}C_R + 0 = 60$$

$$\Delta R_P = \int_{AB+BC} C_R \mathrm{d}P = \int_{AB} C_R \mathrm{d}P + \int_{BC} C_R \mathrm{d}P = 0 + \int_{600}^{650} 0.3 \mathrm{d}P = 15$$

3) L=AD+DC. The equation for AD is C_R = 0.2, $600 \le P \le 650$ and is P = 650, $0.2 \le C_R \le 0.3$ for DC. ΔR_P and ΔR_{C_R} are evaluated as:

$$\Delta R_{C_R} = \int_{AD+DC} P \mathrm{d}C_R = \int_{AD} P \mathrm{d}C_R + \int_{DC} P \mathrm{d}C_R = 0 + \int_{0.2}^{0.3} 650 \mathrm{d}C_R = 65$$

$$\Delta R_P = \int_{AD+DC} C_R \mathrm{d}P = \int_{AD} C_R \mathrm{d}P + \int_{DC} C_R \mathrm{d}P = \int_{600}^{650} 0.2 \mathrm{d}P + 0 = 10$$

As expected, the sum of ΔR_P and ΔR_{CR} persistently equals ΔR although ΔR_P and ΔR_{CR} varies with L.

Appendix D: Mathematical proof of the path-averaged sensitivity

If the interval [x_0, x_N] in Fig. 3 is partitioned into N distinct bins of the same width $\Delta x_i = \Delta x/N$. Eq. (3a) can then be rewritten as:

$$\Delta Z_x = \int_L f_x(x,y)\mathrm{d}x = \lim_{\tau\to 0}\sum_{i=0}^{N-1} f_x(x_i,y_i)\Delta x_i = \lim_{\tau\to 0} N\Delta x_i \frac{\sum_{i=0}^{N-1} f_x(x_i,y_i)}{N} = \Delta x \lim_{\tau\to 0}\frac{\sum_{i=0}^{N-1} f_x(x_i,y_i)}{N} = \overline{\lambda_x}\Delta x$$

where $\overline{\lambda_x} = \lim_{\tau\to 0}\frac{\sum_{i=1}^{N} f_x(x_i,y_i)}{N}$, denoting the average of $f_x(x, y)$ along the curve L. Likewise, we have $\Delta Z_y = \overline{\lambda_y}\Delta y$, where $\overline{\lambda_y}$ denotes the average of $f_y(x, y)$ along the curve L. As a result:

$$\Delta Z = \overline{\lambda_x}\Delta x + \overline{\lambda_y}\Delta y \qquad \text{(D1)}$$

The result can readily be extended to a function of three variables. Applying the mathematic derivation determined above to the MCY equation results in a precise form of Eq. (7):

$$\Delta R = \Delta R_P + \Delta R_{E_0} + \Delta R_n = \overline{\lambda_P}\Delta P + \overline{\lambda_{E_0}}\Delta E_0 + \overline{\lambda_n}\Delta n, \qquad \text{(D2)}$$

where $\Delta R_P = \overline{\lambda_P}\Delta P$, $\Delta R_{E_0} = \overline{\lambda_{E_0}}\Delta E_0$, $\Delta R_n = \overline{\lambda_n}\Delta n$, and $\overline{\lambda_P}$, $\overline{\lambda_{E_0}}$ and $\overline{\lambda_n}$ denote the arithmetic mean of $\partial R/\partial P$, $\partial R/\partial E_0$, and $\partial R/\partial n$ along a path of climate and catchment changes, respectively. Because $\overline{\lambda_P} = \Delta R_P / \Delta P$, $\overline{\lambda_{E_0}} = \Delta R_{E_0} / \Delta E_0$, and $\overline{\lambda_n} = \Delta R_n / \Delta n$, $\overline{\lambda_P}$, $\overline{\lambda_{E_0}}$ and $\overline{\lambda_n}$ also imply the runoff change due to a unit change in P, E_0 and n, respectively.

Appendix E: Path-averaged sensitivity in one-dimensional cases

Given a one-dimensional function z=f(x) and its derivative $f'(x)$. We assumed that $f'(x)$ averages $\overline{\lambda_x}$ over the range $(x, x+\Delta x)$, *i.e.* $\overline{\lambda_x} = \lim_{\tau \to 0} \frac{\sum_{i=1}^{N} f'(x_i)}{N}$. According to the mean value theorem for integrals, $\overline{\lambda_x} = \int_{x}^{x+\Delta x} f'(x) \mathrm{d}x / \Delta x$. In terms of the Newton-Leibniz formula, $\int_{x}^{x+\Delta x} f'(x) \mathrm{d}x = f(x+\Delta x) - f(x) = \Delta \mathrm{z}$. Thus, we obtain: $\overline{\lambda_x} = \Delta \mathrm{z} / \Delta x$.

Acknowledgments

This work was funded by the National Natural Science Foundation of China (41671278), the GDAS' Project of Science and Technology Development (2019GDASYL-0103043) and (2019GDASYL-0502004). I thank Mr. Y.Q. Zheng for his assistance with the mathematic derivations.

References

Barnett, T. P., Pierce, D. W., Hidalgo, H. G., Bonfils, C., Santer, B. D., Das, T., .Bala G., Woods, A. W., Nozawa, T., Mirin, A. A., Cayan D. R., and M. D. Dettinger: Human-induced changes in the hydrology of the western United States. Science, 319(5866), 1080-1083. https://doi.org/10.1126/science.1152538, 2008.

Berghuijs, W. R., R. A. Woods: Correspondence: Space-time asymmetry undermines water yield assessment. Nature Communications 7, 11603. https://doi.org/ 10.1038/ncomms11603, 2016.

Binley, A. M., Beven, K. J., Calver, A., and L. G. Watts: Changing responses in hydrology: assessing the uncertainty in physically based model predictions. Water Resources Research, 27(6), 1253-1261. https://doi.org/10.1029/91WR00130, 1991.

Brown, A. E., Zhang, L., McMahon, T. A., Western, A. W. and R. A Vertessy: A review of paired catchment studies for determining changes in water yield resulting from alterations in vegetation. Journal of Hydrology, 310, 26–61. https://doi.org/ 10.1016/j.jhydrol.2004.12.010, 2005.

Budyko, M. I.: Climate and Life. Academic, N. Y. 1974.

Carmona, A. M., Sivapalan, M., Yaeger, M. A., and Poveda, G.: Regional patterns of interannual variability of catchment water balances across the continental US: A Budyko framework. Water Resources Research, 50, 9177–9193. https://doi:10.1002/2014wr016013, 2014.

Choudhury, B. J.: Evaluation of an empirical equation for annual evaporation using field observations and results from a biophysical model. Journal of Hydrology, 216, 99–110. https://doi.org/10.1016/S0022-1694(98)00293-5, 1999.

Dey, P., and A. Mishra: Separating the impacts of climate change and human activities on streamflow: A review of methodologies and critical assumptions. Journal of Hydrology, 548, 278-290. https://doi.org/10.1016/j.jhydrol.2017.03.014, 2017.

Donohue, R. J., M. L. Roderick, and T. R. McVicar: On the importance of including vegetation dynamics in Budyko's hydrological model. Hydrology and Earth System Sciences, 11, 983–995. https://doi.org/10.5194/hess-11-983-2007, 2007.

Gao, G., Ma, Y., and B. Fu: Multi-temporal scale changes of streamflow and sediment load in a loess hilly watershed of China. Hydrological Processes, 30(3), 365-382, 10.1002/hyp.10585, 2016.

Gasser, T., M. Kechiar, P. Ciais, E. J. Burke, T. Kleinen, D. Zhu, Y. Huang, A. Ekici, and M. Obersteiner: Path-dependent reductions in CO_2 emission budgets caused by permafrost carbon release. Nature Geoscience, 11, 830–835. https://doi.org/ 10.1038/s41561-018-0227-0, 2018.

Jiang, C., Xiong, L., Wang, D., Liu, P., Guo, S., and Xu C.: Separating the impacts of climate change and human activities on runoff using the Budyko-type equations with time-varying parameters. Journal of Hydrology, 522, 326-338, 10.1016/j.jhydrol.2014.12.060, 2015.

Li, Z., Ning, T., Li, J., and D. Yang: Spatiotemporal variation in the attribution of streamflow changes in a catchment on China's Loess Plateau. Catena, 158:1–8. https://doi.org/10.1016/j.catena.2017.06.008, 2017.

Liang, W., D. Bai, F. Wang, B. Fu, J. Yan, S. Wang, Y. Yang, D. Long, and M. Feng: Quantifying the impacts of climate change and ecological restoration on streamflow changes based on a Budyko hydrological model in China's Loess Plateau. Water Resources Research, 51, 6500–6519. https://doi.org/10.1002/ 2014WR016589, 2015.

Liu, J., Zhang, Q., Singh, V. P., and P. Shi. Contribution of multiple climatic variables and human activities to streamflow changes across China. Journal of Hydrology, 545, 145-162. https://doi.org/10.1016/j.jhydrol.2016.12.016, 2016.

Mezentsev, V. S.: More on the calculation of average total evaporation. Meteorol. Gidrol., 5, 24–26, 1955.

Ning, T., Li, Z., and W. Liu: Vegetation dynamics and climate seasonality jointly control the interannual catchment water balance in the Loess Plateau under the Budyko framework, Hydrology and Earth System Sciences, 21, 1515-1526. https://doi.org/10.5194/hess-2016-484, 2017.

Roderick, M. L., and G. D. Farquhar: A simple framework for relating variations in runoff to variations inclimatic conditions and catchment properties. Water Resources Research, 47, W00G07, https://doi.org/10.1029/2010WR009826, 2011.

Sankarasubramanian, A., R. M. Vogel, and J. F. Limbrunner: Climate elasticity of streamflow in the United States. Water Resources Research, 37(6), 1771-1781. https://doi.org/10.1029/2000WR900330, 2001.

Schaake, J. C.: From climate to flow. Climate Change and U.S. Water Resources, edited by P. E. Waggoner, chap. 8, pp. 177 – 206, John Wiley, N. Y. 1990.

Sivapalan, M., Yaeger, M. A., Harman, C. J., Xu, X. Y., and P. A. Troch: Functional model of water balance variability at the catchment scale: 1. Evidence of hydrologic similarity and space-time symmetry, Water Resources Research, 47, W02522, doi:10.1029/2010wr009568, 2011.

Sposito, G.: Understanding the Budyko equation. Water, 9(4), 236. https://doi.org/10.3390/w9040236, 2017.

Sun, Y., Tian, F., Yang, L., and H. Hu: Exploring the spatial variability of contributions from climate variation and change in catchment properties to streamflow decrease in a mesoscale basin by three different methods. Journal of Hydrology, 508(2), 170-180,

https://doi.org/10.1016/j.jhydrol.2013.11.004, 2014.
Wang, D., and M. Hejazi: Quantifying the relative contribution of the climate and direct human impacts on mean annual streamflow in the contiguous United States. Water Resources Research, 47, W00J12, https://doi.org/10.1029/2010WR010283, 2011.
Wang, W., Q. Shao, T. Yang, S. Peng, W. Xing, F. Sun, and Y. Luo: Quantitative assessment of the impact of climate variability and human activities on runoff changes: A case study in four catchments of the Haihe River basin, China. Hydrological Processes, 27(8), 1158–1174. https://doi.org/10.1002/hyp.9299, 2013.
Wu, J., Miao, C., Wang, Y., Duan, Q., and X. Zhang: Contribution analysis of the long-term changes in seasonal runoff on the Loess Plateau, China, using eight Budyko-based methods. Journal of hydrology, 545, 263-275. https://doi.org/10.1016/j.jhydrol.2016.12.050, 2017a.
Wu, J., Miao, C., Zhang, X., Yang, T., and Q. Duan: Detecting the quantitative hydrological response to changes in climate and human activities. Science of the Total Environment, 586, 328-337. https://doi.org/10.1016/j.scitotenv.2017.02.010, 2017b.
Xu, X., Yang, D., Yang, H. and Lei, H.: Attribution analysis based on the Budyko hypothesis for detecting the dominant cause of runoff decline in Haihe basin. Journal of Hydrology, 510: 530-540. http://dx.doi.org/10.1016/j.jhydrol.2013.12.052, 2014.
Yang, H., D. Yang, Z. Lei, and F. Sun: New analytical derivation of the mean annual water-energy balance equation. Water Resources Research, 44, W03410. https://doi.org/10.1029/2007WR006135, 2008.
Yang, H., and D. Yang: Derivation of climate elasticity of runoff to assess the effects of climate change on annual runoff. Water Resources Research, 47, W07526. https://doi.org/10.1029/2010WR009287, 2011.
Yang, H., D. Yang, and Q. Hu: An error analysis of the Budyko hypothesis for assessing the contribution of climate change to runoff. Water Resources Research, 50, 9620–9629. https://doi.org/10.1002/ 2014WR015451, 2014.
Zhao, Q. L., Liu, X. L., Ditmar, P., Siemes, C., Revtova, E., Hashemi-Farahani, H., and R. Klees: Water storage variations of the Yangtze, Yellow, and Zhujiang river basins derived from the DEOS Mass Transport (DMT-1) model. Science China-Earth Sciences, 54, 667-677. https://doi.org/10.1007/s11430-010-4096-7, 2011.
Zhang, S., H. Yang, D. Yang, and A. W. Jayawardena: Quantifying the effect of vegetation change on the regional water balance within the Budyko framework. Geophysical Research Letters, 43, 1140–1148. https://doi.org/10.1002/2015GL066952, 2016.
Zhang, L., Dawes, W. R. and G. R. Walker: Response of mean annual evapotranspiration to vegetation changes at catchment scale. Water Resources Research 37, 701–708. doi; 10.1029/2000WR900325, 2001.
Zhang, L., F. Zhao, A. Brown, Y. Chen, A. Davidson, and R. Dixon: Estimating Impact of Plantation Expansions on Streamflow Regime and Water Allocation. CSIRO Water for a Healthy Country, Canberra, Australia. 2010.
Zhang, L., F. Zhao, Y. Chen, and R. N. M. Dixon: Estimating effects of plantation expansion and climate variability on streamflow for catchments in Australia. Water Resources Research, 47, W12539, https://doi.org/10.1029/2011WR010711, 2011.

Zheng, H., L. Zhang, R. Zhu, C. Liu, Y. Sato, and Y. Fukushima: Responses of streamflow to climate and land surface change in the headwaters of the Yellow River Basin. Water Resources Research, 45, W00A19. https://doi.org/10.1029/2007WR006665, 2009.

Zhou, S., B. Yu, L. Zhang, Y. Huang, M. Pan, and G. Wang (2016), A new method to partition climate and catchment effect on the mean annual runoff based on the Budyko complementary relationship. Water Resources Research, 52, 7163–7177. https://doi.org/10.1002/2016WR019046, 2016.

Table 1. Summary of the long-term hydrometeorological characteristics of the selected catchments[a]

Catchment No.[b]	Area ($10^6 m^2$)	R	P	E_0	n	AI	Reference Period	Evaluation Period	The final Subperiod
1	391	218	1014	935	3.5	0.92	1933-1955	1956-2008	1998-2008
2	16.64	32.9	634	1087	3.16	1.71	1979-1984	1985-2008	1999-2008
3	559	183	787	780	2.68	0.99	1960-1978	1979-2000	1993-2000
4	606	73	729	998	3.07	1.37	1971-1995	1996-2009	2003-2009
5	760	77.9	689	997	2.66	1.45	1970-1995	1996-2009	2003-2009
6	502	57.2	730	988	3.59	1.35	1974-1995	1996-2008	1996-2008
7	673	431	1013	953	1.34	0.94	1947-1955	1956-2008	1998-2008
8	390	139	840	1021	2.61	1.22	1966-1980	1981-2005	1995-2005
9	1130	20.7	633	1077	3.79	1.7	1972-1982	1983-2007	1997-2007
~~10~~	~~3.2~~	~~37.5~~	~~631~~	~~954~~	~~3.49~~	~~1.51~~	~~1989-1991~~	~~1992-2009~~	~~1999-2009~~
~~11~~	~~1.95~~	~~111~~	~~767~~	~~901~~	~~3.06~~	~~1.18~~	~~1990-1992~~	~~1993-2005~~	~~1993-2005~~
~~12~~10	89	272	963	826	2.82	0.86	1958-1965	1966-1999	1987-1999
~~13~~11	243	38.5	735	1010	4.27	1.37	1989-1995	1996-2007	1996-2007
~~14~~12	56.35	65.8	744	1007	3.35	1.35	1989-1995	1996-2008	1996-2008
~~15~~13	14484	385	893	1022	1.11	1.14	1970-1989	1990-2000	1990-2000
~~16~~14	38625	461	985	1087	1.03	1.1	1970-1989	1990-2000	1990-2000
~~17~~15	59115	388	897	1161	1.02	1.29	1970-1989	1990-2000	1990-2000
~~18~~16	95217	371	881	1169	1.03	1.33	1970-1989	1990-2000	1990-2000
~~19~~17	121,972	171	507	768	1.17	1.52	1960-1990	1991-2000	1991-2000
~~20~~18	106,500	60.5	535	905	2.25	1.69	1960-1970	1971-2009	1999-2009
~~21~~19	5891	34.4	506	964	2.54	1.91	1952-1996	1997-2011	2004-2011

[a]R, P, and E_0 represent the mean annual runoff, precipitation and potential evaporation, all in 10^{-3}m yr^{-1}. n (dimensionless) is the parameter representing catchment properties in the MCY equation. AI is the dimensionless aridity index ($AI = E_0/P$). Data of Catchments 1-~~14~~ 12 were derived from Zhang *et al.* (2010). Data of Catchments ~~15~~13-~~18~~ 16 were from Sun *et al.* (2014). Data of Catchments ~~19~~17-~~21~~ 19 were from Zheng *et al.* (2009), Jiang *et al.* (2015), and Gao *et al.* (2016), respectively. I used the change points given in the literatures to divide the observation period into the reference and elevation periods. The LI method further divides the evaluation period into a number of subperiods. The column "The

设置了格式: 字体: 非加粗, 非倾斜
设置了格式: 字体: 非加粗, 非倾斜
设置了格式: 字体: 非加粗, 非倾斜
设置了格式: 字体: 非加粗, 非倾斜
设置了格式: 字体: 非加粗, 非倾斜
设置了格式: 字体: 非加粗, 非倾斜
设置了格式: 字体: 非加粗, 非倾斜
设置了格式: 字体: 非加粗, 非倾斜
设置了格式: 字体: 非加粗, 非倾斜
设置了格式: 字体: 非加粗, 非倾斜
设置了格式: 字体: 非加粗, 非倾斜
设置了格式: 字体: 非加粗, 非倾斜
设置了格式: 字体: 非加粗, 非倾斜
设置了格式: 字体: 非加粗, 非倾斜
设置了格式: 字体: 非加粗, 非倾斜
设置了格式: 字体: 非加粗, 非倾斜
设置了格式: 字体: 非加粗, 非倾斜
设置了格式: 字体: 非加粗, 非倾斜

final Subperiod” denotes the final subperiod, which was used as the evaluation period for the total differential method, the decomposition method and the complementary method.~~ The bold and italic rows denote that the column “Evaluation Period” is the same as the column “The final Subperiod”.~~

[b]Catchments 1-~~14~~ 12 are in Australia and the others are in China. 1: Adjungbilly CK; 2: Batalling Ck; 3: Bombala River; 4: Crawford River; 5: Darlot Ck; 6: Eumeralla River; 7: Goobarragandra CK; 8: Jingellic CK; 9: Mosquito CK; ~~10: Pine Ck; 11: Red Hill;~~ ~~12~~10: Traralgon Ck; ~~13~~11: Upper Denmark River; ~~14~~12: Yate Flat Ck; ~~15~~13: Yangxian station, Hang River; ~~16~~14: Ankang station, Hang River; ~~17~~15: Baihe station, Hang River; ~~18~~16: Danjiangkou station, Hang River; ~~19~~17: Headwaters of the Yellow River Basin; ~~20~~18: Wei River; ~~21~~19: Yan River.

Table 2. Comparisons of R (mm yr^{-1}), P (mm yr^{-1}), E_0 (mm yr^{-1}), and n (dimensionless) between the reference and the evaluation periods[a]

Catchment No.	R_1	R_2	P_1	P_2	E_{01}	E_{02}	n_1	n_2	ΔR	ΔP	ΔE_0	Δn
1	223	216	959	1038	950	928	2.7	4.1	-7.2	79.2	-21	1.4
2	40.6	31	655	629	1087	1087	3	3.2	-9.7	-27	0	0.2
3	249	127	847	736	780	780	2.3	3.2	-122	-112	0.4	0.9
4	90.6	41.5	753	685	1002	989	2.9	3.7	-49	-67	-13	0.8
5	94.9	46.3	718	633	1000	992	2.5	3	-49	-85	-9	0.5
6	70.8	34.3	756	687	989	987	3.4	4.1	-36	-69	-2	0.6
7	575	406	1123	995	931	957	1.1	1.4	-169	-128	25	0.3
8	139	139	871	821	1043	1008	2.7	2.5	-0.4	-50	-35	-0.2
9	24.1	19.2	659	621	1100	1067	3.7	3.8	-4.9	-37	-33	0.1
~~10~~	~~116~~	~~24.3~~	~~588~~	~~638~~	~~927~~	~~958~~	~~1.7~~	~~4.2~~	~~-92~~	~~50.4~~	~~31~~	~~2.5~~
~~11~~	~~297~~	~~68~~	~~986~~	~~716~~	~~884~~	~~905~~	~~2.3~~	~~3.6~~	~~-229~~	~~-271~~	~~22~~	~~1.3~~
10~~12~~	301	265	992	956	820	828	2.7	2.8	-36	-36	7.4	0.1
11~~13~~	48.5	32.6	752	725	991	1021	4.2	4.4	-16	-28	30	0.2
12~~14~~	90.4	52.6	753	739	991	1015	2.9	3.7	-38	-14	24	0.8
13~~15~~	435	295	948	795	1008	1047	1.1	1.2	-139	-153	38	0.1
14~~16~~	520	353	1035	894	1074	1109	1	1.2	-167	-141	35	0.2
15~~17~~	441	291	939	820	1149	1182	1	1.2	-151	-119	33	0.2
16~~18~~	412	296	913	821	1163	1179	1	1.1	-116	-92	15	0.2
17~~19~~	180	144	512	491	774	751	1.1	1.3	-36	-21	-23	0.2
18~~20~~	90.2	52.1	585	520	895	908	2.1	2.3	-38	-65	13	0.2
19~~21~~	37.7	24.6	521	462	954	995	2.6	2.5	-13	-59	41	~~0~~-0.1

[a]The subscript "1" denotes the reference period and "2" denotes the evaluation period. $\Delta X = X_2 - X_1$ (X as a substitute for R, P, E_0, and n).

设置了格式: 突出显示

设置了格式: 突出显示

设置了格式: 突出显示

设置了格式: 突出显示

Table 3. Effects of precipitation (ΔR_P, 10^{-3}m yr^{-1}), potential evapotranspiration (ΔR_{E_0}, 10^{-3}m yr^{-1}), and catchment changes (ΔR_n, 10^{-3}m yr^{-1}) on the mean annual runoff determined from the four evaluated methods

Catchment NO.[a]	LI Method			Decomposition Method	Total Differential Method			Complementary Method		
	ΔR_P	ΔR_{E_0}	ΔR_n	ΔR_n	ΔR_P	ΔR_{E_0}	ΔR_n	ΔR_P	ΔR_{E_0}	ΔR_n
1	-70.9	-8.99	-24.3	-44.6	-67	4.82	-62	-60.7	4.34	-47.3
2	-6.49	0.95	-9.74	-9.65	-7.2	1.3	-13	-6.23	1.13	-10.2
3	-89	25.9	-140	-128	-104	26.6	-483	-88	25.7	-140
4	-18.1	2.09	-35.4	-36.3	-18	2.37	-58	-14.8	1.99	-38.5
5	-27.9	1.14	-21.3	-18.6	-34	1.18	-27	-28.1	0.97	-20.9
6	-19.9	0.29	-16.7	-14.9	-24	0.36	-22	-19.9	0.29	-16.7
7	-211	-7.19	-101	-90.9	-236	-6.9	-134	-211	-6.21	-102
8	-32.2	12.3	-14.4	-12.6	-35	12.6	-15	-32.9	11.9	-13.3
9	-11.8	3.02	-9.96	-8.45	-13	0.85	-20	-8.76	0.56	-10.5
~~10~~	~~19.47~~	~~-5.61~~	~~-119~~	~~-96.5~~	~~0.91~~	~~-10~~	~~-291~~	~~0.56~~	~~-6.53~~	~~-99.1~~
~~11~~	~~-150~~	~~-7.46~~	~~-71.8~~	~~-60.7~~	~~-188~~	~~-9.4~~	~~-113~~	~~-144~~	~~-7.04~~	~~-78.3~~
10~~12~~	-9.88	-3.99	-79.2	-82	-11	-0.5	-154	-10.8	-0.57	-81.6
11~~13~~	-6.98	-4.36	-4.54	-4.21	-8	-5.1	-5.2	-7	-4.38	-4.51
12~~14~~	-4.84	-4.42	-28.7	-27.9	-5.6	-5	-37	-4.85	-4.4	-28.6
13~~15~~	-104	-8.56	-24.8	-23	-110	-9.4	-27	-103	-8.52	-25.1
14~~16~~	-99.3	-7.99	-58.8	-56	-105	-8.3	-68	-99	-7.92	-59.1
15~~17~~	-78.8	-6.26	-63.9	-61	-84	-6.5	-76	-78.6	-6.2	-64.2
16~~18~~	-60.1	-2.79	-53.5	-52	-64	-2.9	-62	-60	-2.77	-53.6
17~~19~~	-11.9	3.89	-27.6	-27	-12	3.81	-31	-11.9	3.85	-27.5
18~~20~~	-27.5	-2.46	-18.5	-17	-31	-4.4	-26	-25.5	-3.47	-19.5
19~~21~~	-10.4	-3.47	-2.11	-3.4	-9.9	-4.8	-4.8	-8.27	-3.86	-3.82

[a]~~The bold and italic numbers denote that the evaluation period comprises a single subperiod.~~

设置了格式: 字体: 非加粗, 非倾斜
设置了格式: 字体: 非加粗, 非倾斜
设置了格式: 字体: 非加粗
设置了格式: 字体: 非加粗, 非倾斜
设置了格式: 字体: 非加粗
设置了格式: 字体: 非加粗, 非倾斜
设置了格式: 字体: 非加粗
设置了格式: 字体: 非加粗, 非倾斜
设置了格式: 字体: 非加粗
设置了格式: 字体: 非加粗, 非倾斜
设置了格式: 字体: 非加粗
设置了格式: 字体: 非加粗, 非倾斜
设置了格式: 字体: 非加粗
设置了格式: 字体: 非加粗, 非倾斜
设置了格式: 字体: 非加粗
设置了格式: 字体: 非加粗, 非倾斜

~~**Table 4.** Comparisons of the path-averaged sensitivities with the point sensitivities of runoff~~ [a, b]

Catchment NO.	$\overline{\lambda_P}$	$\overline{\lambda_{E0}}$	$\overline{\lambda_n}$	λ_{Pf}	λ_{E0f}	λ_{nf}
1	0.68	-0.55	-17	0.621	-0.39	-71.8
2	0.2	-0.08	-27.3	0.227	-0.1	-30.9
3	0.58	-0.36	-26.7	0.68	-0.42	-79
4	0.3	-0.16	-30.5	0.39	-0.2	-50.1
5	0.33	-0.14	-43.1	0.394	-0.19	-59.4
6	0.29	-0.16	-26.5	0.352	-0.2	-34.9
7	0.71	-0.32	-223	0.781	-0.33	-299
8	0.49	-0.26	-77.9	0.478	-0.27	-64.9
9	0.16	-0.07	-11.8	0.161	-0.07	-17.6
10	0.27	-0.12	-40.9	0.45	-0.16	-99.9
11	0.55	-0.35	-56.1	0.695	-0.44	-88.2
12	0.72	-0.45	-57.3	0.74	-0.53	-61.1
13	0.25	-0.15	-19.8	0.29	-0.17	-22.5
14	0.34	-0.18	-37.2	0.393	-0.21	-48.6
15	0.68	-0.22	-275	0.719	-0.25	-303
16	0.7	-0.23	-326	0.745	-0.24	-378
17	0.66	-0.19	-320	0.708	-0.2	-378
18	0.65	-0.19	-315	0.692	-0.19	-363
19	0.58	-0.17	-153	0.602	-0.17	-175
20	0.32	-0.12	-50.1	0.402	-0.16	-69.6
21	0.2	-0.06	-29.2	0.234	-0.09	-34

~~[a] $\overline{\lambda_P}$ (10^{-3}m10^{-3}m^{-1}), $\overline{\lambda_{E0}}$ (10^{-3}m 10^{-3}m^{-1}), and $\overline{\lambda_n}$ (dimensionless) represent the path-averaged sensitivities of runoff to precipitation, potential evaporation, and catchment properties (see Appendix D). If the evaluation period comprised only one subperiod, $\overline{\lambda_P}$, $\overline{\lambda_{E0}}$ and $\overline{\lambda_n}$ was calculated as: $\overline{\lambda_P} = \Delta R_P / \Delta P$,~~

设置了格式: 突出显示
设置了格式: 突出显示
设置了格式: 突出显示
设置了格式: 突出显示
设置了格式: 突出显示
设置了格式: 突出显示
设置了格式: 突出显示
设置了格式: 突出显示
设置了格式: 突出显示
设置了格式: 突出显示

~~$\overline{\lambda_{E_0}} = \Delta R_{E_0} / \Delta E_0$, and $\overline{\lambda_n} = \Delta R_n / \Delta n$. If the evaluation period comprised N>1 subperiods, the equations became: $\overline{\lambda_P} = \sum_{i=1}^{N} |\Delta R_{Pi}| / \sum_{i=1}^{N} |\Delta P_i|$; $\overline{\lambda_{E_0}} = -\sum_{i=1}^{N} |\Delta R_{E0i}| / \sum_{i=1}^{N} |\Delta E_{0i}|$, and $\overline{\lambda_n} = -\sum_{i=1}^{N} |\Delta R_{ni}| / \sum_{i=1}^{N} |\Delta n_i|$, where the subscript i denotes the ith subperiod.~~

~~[b] λ_P, λ_{E0}, and λ_n represent the point sensitivities of runoff of the total differential method , which was calculated by substituting the observed mean annual values of the reference period into Eq. (2).~~

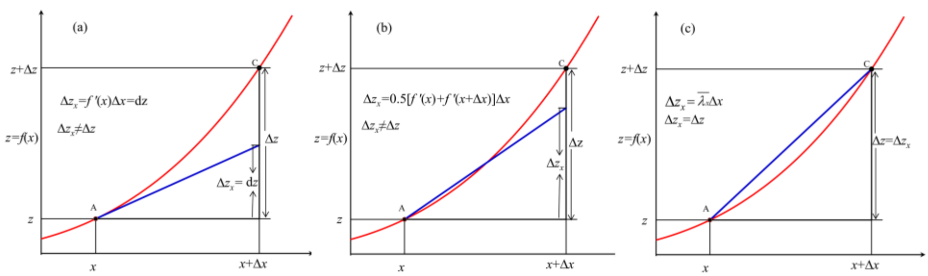

Fig. 1. For a non-linear function $z= f(x)$, the total differential method (a) and the complementary method (b) fails to accurately estimate the effect (Δz_x) of x on z when x changes by Δx, but the LI method (c) does. For a univariate function, the z change is exclusively driven by x, so that Δz_x should be equal to Δz. $\Delta z_x = \Delta z$ in (c) but not in (a) and (b). $\overline{\lambda_x}$ in (c) represents the average sensitivity along the curve AC and $\overline{\lambda_x} = \Delta z / \Delta x$, see Appendix E for details.

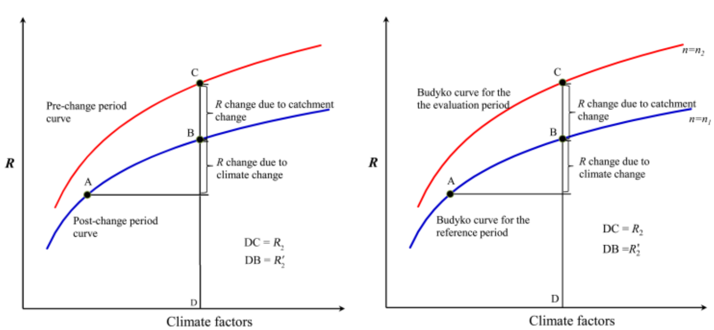

Fig. 2. A schematic plot to illustrate the decomposition method. Pont A denotes the initial state (the reference period) and Point C denotes the terminal state (the evaluation period). R_2 represents the mean annual runoff of the evaluation period, and $R_2^{'}$ the mean annual runoff given the climate conditions of the evaluation period and the catchment conditions of the reference period. See Section 2.4 for details.

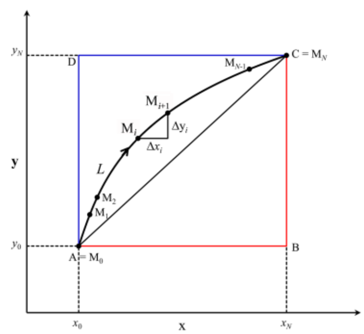

Fig. 3. A schematic plot illustrating the LI method.

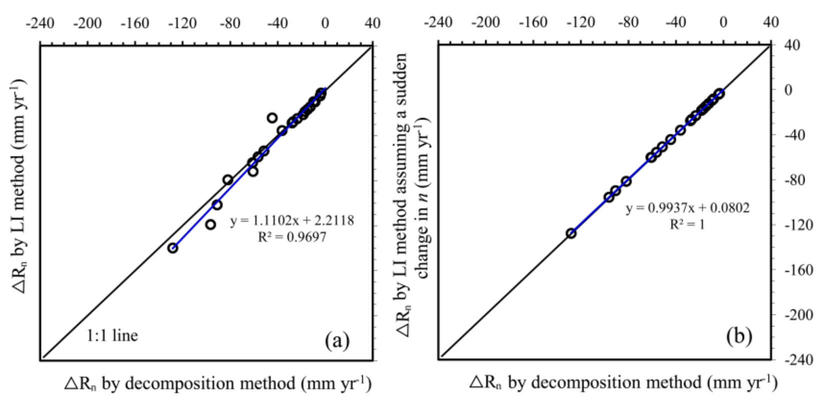

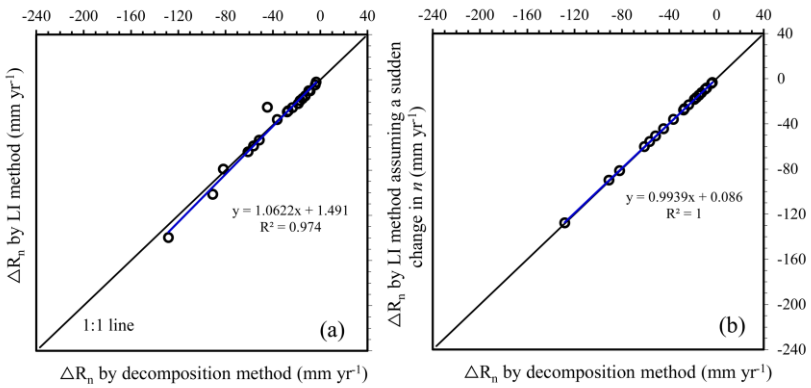

Fig. 4. Comparisons between the LI method and the decomposition method. (a) Comparison of the estimated contributions to the runoff changes from the catchment changes (ΔR_n); (b) the decomposition method is equivalent to the LI method that assumes a sudden change in catchment properties following climate change. In this case, the integral path of the LI method can be considered as the~~ broken~~ ~~line~~path ABC~~ AB+BC~~ in Fig. 3 (x represents climate factors and y catchment properties, *i.e.* n) and $\Delta R_n = \int_{AB+BC} \frac{\partial R}{\partial n} dn = \int_{AB} \frac{\partial R}{\partial n} dn + \int_{BC} \frac{\partial R}{\partial n} dn = 0 + \int_{BC} \frac{\partial R}{\partial n} dn = \int_{n_1}^{n_2} f_n(P_2, E_{02}, n) dn$, where the subscript "1" denotes the reference period and "2" denotes the final subperiod of the evaluation period.

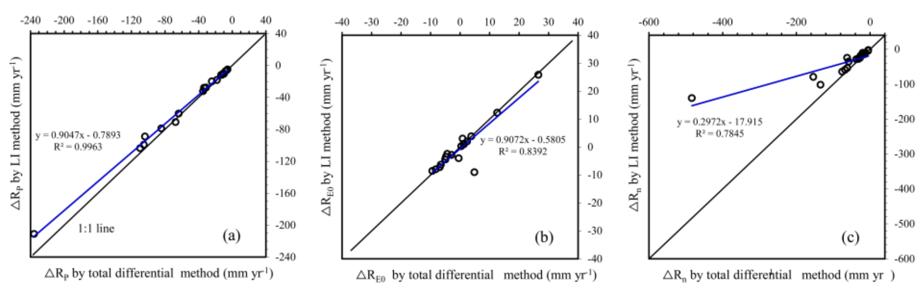

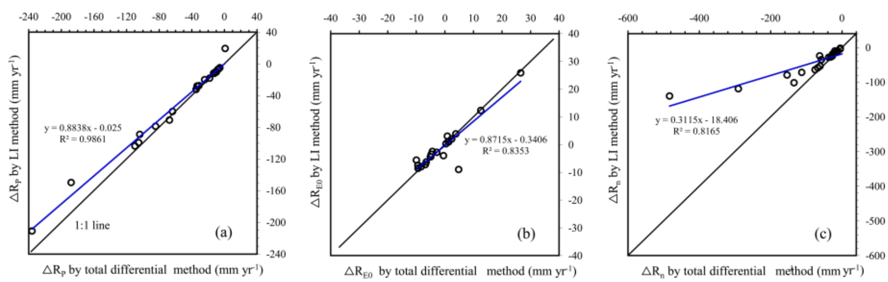

Fig. 5. Comparisons of the estimated contribution to runoff from the changes in (a) precipitation (ΔR_P), (b) potential evapotranspiration (ΔR_{E_0}), and (c) catchment properties (ΔR_n) between the LI method and the total differential method.

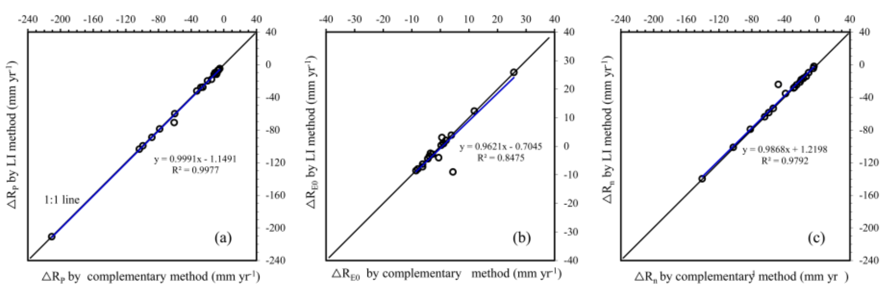

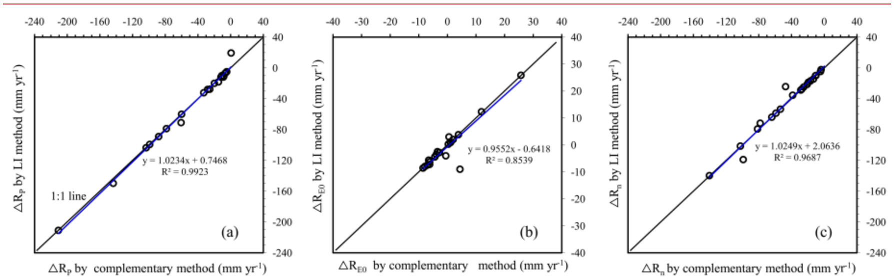

Fig. 6. Comparisons of (a) ΔR_P, (b) ΔR_{E_0}, and (c) ΔR_n between the LI method and the complementary method (a = 0.5).

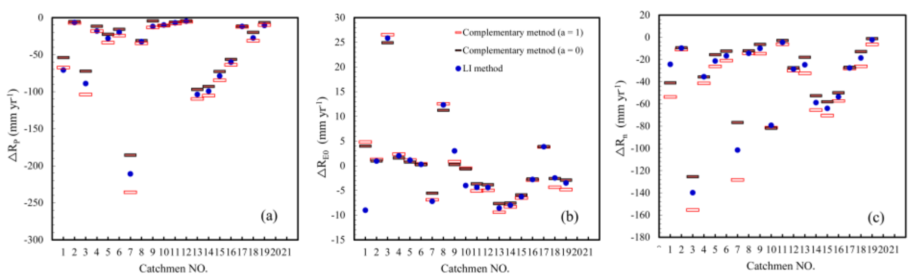

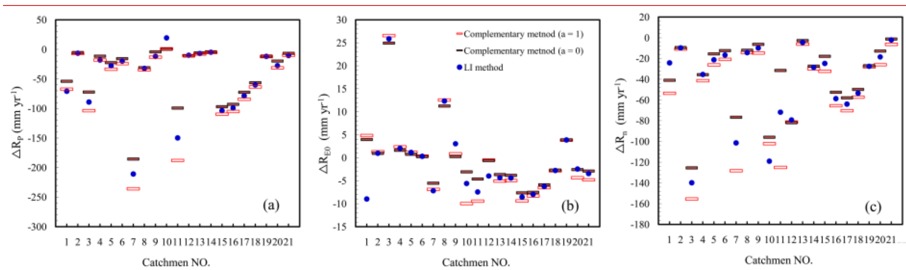

Fig. 7. Comparisons of (a) ΔR_P, (b) ΔR_{E_0}, and (c) ΔR_n by the LI method with the upper ~~(*a*=1)~~ and lower ~~(*a*=0)~~ bounds given by the complementary method. According to Zhou *et al*. (2016), ΔR_P, ΔR_{E_0}, and ΔR_n reach their bounds when *a* is 0 or 1.

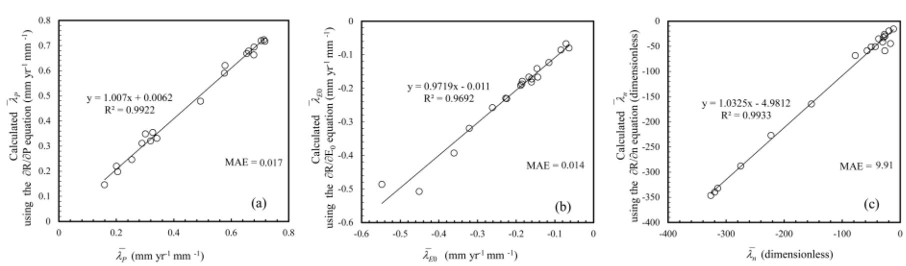

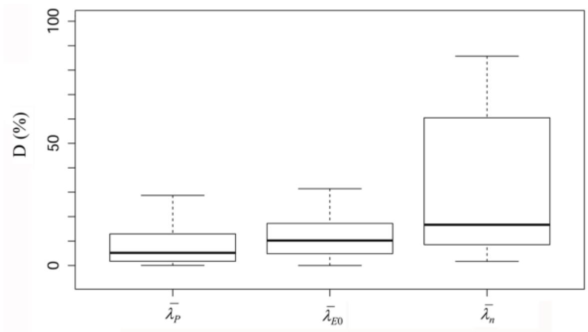

~~**Fig. 8**. Boxplots showing the temporal variability of the path-averaged sensitivities of water yield to precipitation ($\overline{\lambda_P}$), potential evapotranspiration ($\overline{\lambda_{E0}}$), and catchment properties ($\overline{\lambda_n}$). *D* (%) was calculated as the relative difference between the sensitivity of the whole evaluation period and that of a subperiod. In the calculations, I excluded the catchments that had an evaluation period comprising only one subperiod. The boxes span the inter-quartile range (IQR) and the solid lines are medians. The whiskers represent the data range, excluding statistical outliers, which extend more than 1.5IQR from the box ends.~~

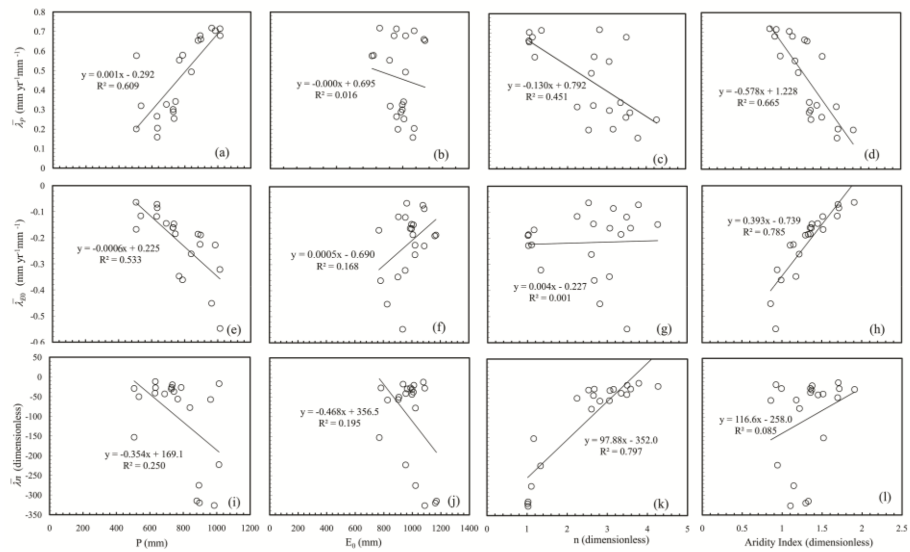

~~Fig. 9. $\overline{\lambda_P}$, $\overline{\lambda_{E0}}$ and $\overline{\lambda_n}$ in correlation with P, E_0, n, and aridity index.~~

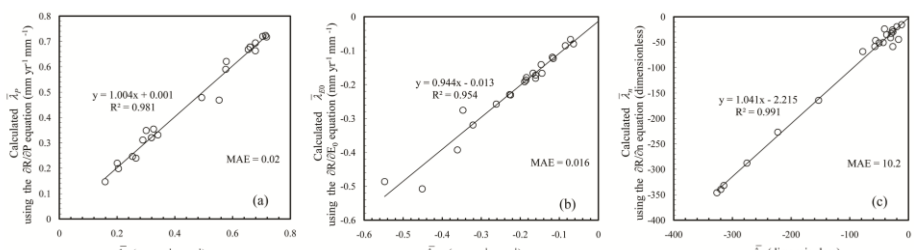

Fig. 8~~10~~. Performances of Eq. (2) to be used to predict $\overline{\lambda_P}$, $\overline{\lambda_{E0}}$ and $\overline{\lambda_n}$ ~~Comparisons of $\overline{\lambda_P}$, $\overline{\lambda_{E0}}$ and $\overline{\lambda_n}$ (given in Table 4) with those predicted using Eq. (2)~~ with the long-term mean values of P, E_0, and n as inputs. $MAE = N^{-1}\sum_{i=1}^{N}|O_i - P_i|$, is the mean absolute error, where O and P are values that actually encountered (given in Table ~~4~~S4) and predicted using Eq. (2) respectively, and N is the number of selected catchments.

域代码已更改

域代码已更改

域代码已更改

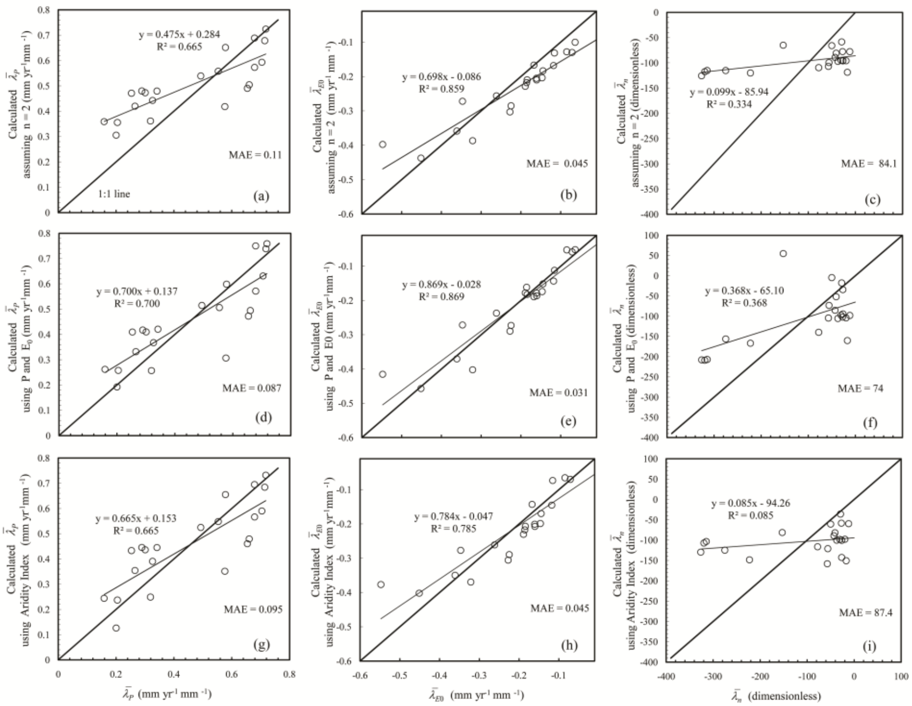

~~**Fig. 11**. Comparisons of~~ $\overline{\lambda_P}$, $\overline{\lambda_{E0}}$ ~~and~~ $\overline{\lambda_n}$ ~~with those predicted by the three strategies. (a)-(c) Predicted by Eq. (2) with a constant *n* (*n* = 2), (d)-(f) predicted by the regression equations established using *P* and *E*~~$_0$~~:~~ $\overline{\lambda_P} = 0.0011P - 0.0006E_0 + 0.21$ ~~(R^2=0.7),~~ $\overline{\lambda_{E0}} = 0.0007P - 0.0007E_0 - 0.38$ ~~(R^2=0.87), and~~ $\overline{\lambda_n} = -0.302P - 0.372E_0 + 493$ ~~(R^2=0.37), and (g)-(i) predicted by the regression equations established using only the aridity index, as shown in Fig. 9 (d), (h) and (l). *MAE* was calculated using the same procedure as in Fig. 10.~~

带格式的: 行距: 单倍行距